# Lyapunov stability of Vlasov equilibria using Fourier-Hermite modes

R. Paškauskas[1,*] and G. De Ninno[1,2]
[1]*Sincrotrone Trieste, Basovizza, 34012 Trieste, Italy*
[2]*University of Nova Gorica, 5001 Nova Gorica, Slovenia*

(Received 10 April 2009; revised manuscript received 3 July 2009; published 9 September 2009)

We propose an efficient method to compute Lyapunov exponents and Lyapunov eigenvectors of long-range interacting many-particle systems, whose dynamics is described by the Vlasov equation. We show that an expansion of a distribution function using Hermite modes (in velocity variable) and Fourier modes (in configuration variable) converges fast if an appropriate scaling parameter is introduced and identified with the inverse of the temperature. As a consequence, dynamics and linear stability properties of many-particle states, both in the close-to and in the far-from equilibrium regimes, can be predicted using a small number of expansion coefficients. As an example of a long-range interacting system we investigate stability properties of stationary states, the Hamiltonian mean-field model.

DOI: 10.1103/PhysRevE.80.036402 PACS number(s): 52.65.Ff, 05.10.−a, 02.70.Dh

## I. INTRODUCTION

In the mean-field limit, the collective dynamics of many-particle systems interacting via long-range forces obeys the Vlasov equation [1–4],

$$\frac{\partial f(x,p,t)}{\partial t} + p\frac{\partial f(x,p,t)}{\partial x} - \frac{\partial \varphi_f(x,t)}{\partial x}\frac{\partial f(x,p,t)}{\partial p} = 0. \quad (1)$$

Here $f(x,p,t)$ is the single-particle density function, while $x$ and $p$ are the particle configuration and momentum coordinates, respectively. The self-field

$$\varphi_f(x,t) = \int K(x-x')\rho_f(x',t)dx' \quad (2)$$

is generated by the particle interaction potential $K(x-x')$ and by the density $\rho_f(x,t)=\int f(x,p,t)dp$.

There is growing evidence that the presence of long-range interactions results in the distribution function being trapped in quasistationary states, different from the thermodynamical equilibrium. In this regime, the nonlinear-dynamical effects become important. For example, the distribution function can be described by a local Lyapunov exponent, derived from the linearization of the Vlasov equation, while a path of transition from an unstable stationary state to a quasistationary state can be identified with the directionality of the unstable manifold. Representing the evolution of the distribution function as a trajectory in a low-dimensional projection can provide new qualitative information about the quasistationary state and allow us to use tools of the qualitative analysis of the low-dimensional dynamical systems [5].

To evolve the distribution function by the Vlasov equation numerically accurately, it is usually important to take into account small scale filamentation effects of the distribution function and therefore a large dimensional projection is needed. The properties of quasistationary states, however, typically are only sensitive to large-scale structures of the distribution function. Effective representation of equilibria and of their local Lyapunov stability is one of the main challenges addressed in this paper. Focusing on one-dimensional systems represented by density functions with Gaussian-like tails in the momentum variable and spatially periodic boundary conditions in the configuration variable, we demonstrate that a Fourier-Hermite expansion of $f(x,p,t)$ can reproduce both the Lyapunov spectrum and Lyapunov eigenvectors with a small number of expansion coefficients. We also show that introducing an appropriate scaling parameter, to be identified with the inverse of the temperature, allows us to significantly improve convergence of the expansion.

As a test model, we investigate stability properties of stationary states of the Hamiltonian mean-field (HMF) model [6,7].

The plan of the paper is as follows. In Sec. II we introduce the Fourier-Hermite expansion of a density function and discuss the scaling parameter. The spectral equation, the Lyapunov spectrum, and the Lyapunov eigenvectors are introduced in Sec. III. Relevant facts about the HMF model are summarized in Sec. IV. Results of our method, applied to the HMF model, are presented in Sec. V. Finally, in Sec. VI, we draw conclusions.

## II. FOURIER-HERMITE EXPANSION

Collective properties of many-body dynamical systems are typically more evident when states are represented in terms of density functions. To evolve the density function in time with sufficient accuracy small scale structures or filaments usually have to be resolved. Lyapunov exponents can be resolved with an alternative and typically low-dimensional projection of the density function in terms of a set of coefficients $\mathbf{a}=\{a_n\}$. The latter projection can be viewed as a map,

$$f(x,p,t) = \Pi(x,p)\mathbf{a}(t), \quad (3)$$

for example, a Galerkin projection [8] of a density function $f(x,p,t)$ to a set of coefficients. For the Vlasov equation, discretization in momentum variable requires careful analysis. Therefore we first consider a partial projection of $f(x,p,t)$,

*rytis.paskauskas@elettra.trieste.it

 

$$f(x,p,t) = \sum_{n\geq 0} a_n(x,t)\sqrt{\hat{\beta}^{\kappa_n}}\Psi_n(\sqrt{\hat{\beta}}p), \tag{4a}$$

$$a_n(x,t) = \frac{1}{\sqrt{\hat{\beta}^{\kappa_n-1}}}\int f(x,p,t)\Psi^n(\sqrt{\hat{\beta}}p)dp. \tag{4b}$$

Here $\{\Psi_n(y)\}_{n\geq 0}$ are basis functions and $\{\Psi^n(y)\}_{n\geq 0}$ are basis weights. They form complete, normalized, adjoint bases, i.e., $\int\Psi^n(y)\Psi_m(y)dy=\delta_{nm}$, for differentiable distributions. We have introduced a free scaling function $\hat{\beta}$, which will be determined later. Since $\hat{\beta}$ is a function of time, derivatives $\partial\dot{a}_n/\partial a_n$ depend on the choice of a free parameter $\kappa_n$. It is possible to fix $\kappa_n$ by requiring that $\partial\dot{a}_n/\partial a_n=0$.

In the following, we make use of the so-called asymmetrically weighted Hermite expansion [9–11] (as opposed to the symmetrically weighted Hermite expansion discussed in [9]) defined by

$$\Psi_n(y) = (2\pi)^{-1/2}(-d/dy)^n \exp(-y^2/2), \tag{5a}$$

$$\Psi^n(y) = (n!)^{-1}\exp(y^2/2)(-d/dy)^n\exp(-y^2/2). \tag{5b}$$

Analysis of the Vlasov equation based on Hermite expansions in momentum has been introduced in [10,11], with the emphasis on the accuracy of numerical solvers.

Advantages of Hermite polynomials include facts that the basis functions decay as $\Psi_n(y)\sim\exp(-y^2/2)$ for large $|y|$, i.e., in accordance with typical physical boundary conditions, and that the recursion relations, relevant for the Vlasov equation, are simple,

$$y\Psi_n = A_n^+\Psi_{n+1} + A_n^-\Psi_{n-1}, \tag{6a}$$

$$\Psi_n' = -B_n^+\Psi_{n+1} + B_n^-\Psi_{n-1}. \tag{6b}$$

In general, the density $\rho_f(x,t)$ can be expressed as $\rho_f(x,t)=\boldsymbol{\alpha}\cdot\mathbf{a}$, where $\boldsymbol{\alpha}=\{\alpha_n\}_{n\geq 0}$, $\alpha_n=\int\Psi_n(y)dy$. In the asymmetrically weighted Hermite basis $\rho_f(x,t)=a_0(x,t)$. Looking at Eq. (2), one can see that in this way the couplings between different momentum modes $a_n$ are minimal. This motivates the choice of the asymmetrically weighted expansion. In this basis, we have $A_n^+=1$, $A_n^-=n$, $B_n^+=1$, $B_n^-=0$, $\kappa_n=n+1$.

Using expansion (4), the Vlasov equation [Eq. (1)] is cast as

$$\frac{d\mathbf{a}}{dt} + \mathbb{V}^-(\mathbf{a})\mathbf{a} + \mathbb{V}^+(\mathbf{a})\mathbf{a} + \mathbb{S}^-(\mathbf{a})\mathbf{a} + \mathbb{S}^+(\mathbf{a})\mathbf{a} = 0, \tag{7}$$

where $\mathbb{V}^\pm(\mathbf{a})$ are defined as

$$\mathbb{V}^\pm_{n,n'}(\mathbf{a}) = \hat{\beta}^{\mp 1/2}\delta_{n\mp 1,n'}\left(\frac{A^\pm_{n'}}{\sqrt{\hat{\beta}}}\frac{\partial}{\partial x} \pm \sqrt{\hat{\beta}}B^\pm_{n'}\frac{\partial}{\partial x}\int K(x-x')\boldsymbol{\alpha}\cdot\mathbf{a}(\mathbf{x}',\mathbf{t})dx'\right), \tag{8}$$

and

$$\mathbb{S}^\pm_{n,n'}(\mathbf{a}) = (\mp)\hat{\beta}^{\mp}B^\pm_{n\mp 2}A^\pm_{n\mp 1}\delta_{n\mp 2,n'} \times \frac{B_1^+\left\langle\frac{\partial\varphi_f}{\partial x}a_1\right\rangle - \hat{\beta}B_3^-\left\langle\frac{\partial\varphi_f}{\partial x}a_3\right\rangle}{\frac{B_0^+A_1^+}{\hat{\beta}}\langle a_0\rangle - \hat{\beta}B_2^-A_1^-\langle a_4\rangle}. \tag{9}$$

Here $\langle\cdot\rangle\equiv\int\cdot dx$. Lyapunov spectrum is obtained by analysis of the linearization of Eq. (7) around an arbitrary reference state $\mathbf{a}_0$ in Sec. III.

The Vlasov dynamics typically proceeds as an interplay between two mechanisms, advection and convection, and there are two scales of spatial variations associated with them. The convection, represented by the nonlinear term in Eq. (1), determines the evolution of the width of the distribution function in momentum variable. It is related to the (time-dependent) temperature $T(t)$,

$$T(t) = \int p^2 f(x,p,t)dxdp. \tag{10}$$

On this scale, transitions between different macroscopic states can be observed. The advection term drives the filamentation process independently. It is characterized by ever thinning of inhomogeneities (filaments) of $f$ down to the scale of fluctuations in the underlying discrete many-particle system.

In order to represent large-scale variations in $f$ efficiently, we focus on the former, the temperature scale. The parameter $\hat{\beta}$ in expansion (4) can be tuned to maximize the content of the lowest order mode $a_0(x,t)$, assumed to be nonzero. Using Eq. (4), one can show that the previous condition is equivalent to

$$\int a_2(x,t)dx = 0, \tag{11}$$

which in turn corresponds to $\hat{\beta}=1/T(t)$. In this way $\hat{\beta}$ becomes a dynamical variable, whose evolution is defined by enforcing Eq. (11). However, for the Lyapunov exponents of a stationary state, derivatives of $\hat{\beta}$, and the two last terms in Eq. (7), can be neglected.

In the rest of this paper we will study Lyapunov spectrum of smooth distributions and periodic boundary conditions in $x$; therefore a Fourier decomposition of $a_n(x,t)$ is adequate,

$$a_n(x,t) = \sum_{m\in\mathbb{Z}}\frac{a_{mn}}{2\pi}\exp(-\imath mx). \tag{12}$$

With expansions (4) and (12), the evolution is provided in terms of the complex coefficients $\mathbf{a}=\{a_{mn}\}$, with $a_{mn}=a^*_{-m,n}$. The Vlasov matrix $\mathbb{V}^\pm$ can be extended to include the expansion in $x$ by noting that the derivative $\partial/\partial x$, acting on $a_{mn}$, is a diagonal operator: $\partial/\partial x=-\imath m$.

For calculations, we use a finite truncation in $N_F\times N_H$ complex coefficients and let $0\leq m\leq N_F$ and $0\leq n<N_H$.

## III. LOCAL LYAPUNOV EXPONENTS

The local stability properties of an arbitrary state $\mathbf{a}_0$ are determined by the properties of the linearization of Eq. (7). The local Lyapunov spectrum $\{\sigma_i\}$ and the corresponding Lyapunov vectors $\{\boldsymbol{\psi}_i\}$ are defined by all solutions $(\sigma, \boldsymbol{\psi})$ of the spectral equation,

$$\sigma\boldsymbol{\psi} = \mathbb{A}(\mathbf{a}_0)\boldsymbol{\psi}. \tag{13}$$

Here $\mathbb{A}$ is the fundamental matrix, defined by

$$\mathbb{A}(\mathbf{a}) = \iota\frac{\partial}{\partial \mathbf{a}}[\mathbb{V}^-(\mathbf{a})\mathbf{a} + \mathbb{V}^+(\mathbf{a})\mathbf{a}]. \tag{14}$$

Investigating the convergence properties of the spectrum as a function of the truncation dimension is one of the central objectives of this paper. The physical interpretation of Eq. (13) follows. On a short time scale, the evolution of a perturbed state $f_\epsilon(0)=\Pi\mathbf{a}(0)+\epsilon\Pi\boldsymbol{\xi}$ (where $\epsilon$ is a small parameter and $\boldsymbol{\xi}$ is an arbitrary vector) can be written as $f_\epsilon(t)\approx\Pi\mathbf{a}(0)+\epsilon\Pi\boldsymbol{\xi}(t)$ to the first order in $\epsilon$. The vector $\boldsymbol{\xi}$ evolves according to the following equation:

$$\boldsymbol{\xi}(t) = \sum_i [\overline{\boldsymbol{\psi}}_i \cdot \boldsymbol{\xi}]\exp(\iota\sigma_i t)\boldsymbol{\psi}_i. \tag{15}$$

Here $\{\overline{\boldsymbol{\psi}}_i\}$ is the adjoint basis to $\{\boldsymbol{\psi}_i\}$, satisfying $\overline{\boldsymbol{\psi}}_i\boldsymbol{\psi}_j=\delta_{ij}$, and $\delta_{ij}$ is the Kronecker delta function. If for some $i$, $\lambda_i \equiv \mathrm{Im}(-\sigma_i) > 0$, then the corresponding eigenvector $\boldsymbol{\psi}_i$ is amplified exponentially in time. It is referred to as an expanding eigenvector. The expansion rate $\lambda_i$ is called the local Lyapunov exponent. The leading local Lyapunov exponent is defined by

$$\lambda = \max_i \mathrm{Im}(-\sigma_i). \tag{16}$$

It controls the rate of the exponential divergence of nearby states in time. The divergence can be approximated by

$$f_\epsilon(x,p,t) \approx f_0(x,p) + (\overline{\boldsymbol{\psi}}\cdot\boldsymbol{\xi})e^{\lambda t}\Pi\boldsymbol{\psi}, \tag{17}$$

where $\boldsymbol{\psi}$ and $\overline{\boldsymbol{\psi}}$ are the expanding eigenvector and its adjoint, respectively, corresponding to the spectral eigenvalue $\sigma$ with $\mathrm{Im}(-\sigma)=\lambda$, and $\lambda$ is the leading local Lyapunov exponent. If all $\sigma_i$ are real, the state is said to be spectrally stable and $\lambda=0$.

The rate of exponential divergence between two distribution functions can be computed by monitoring the evolution of their difference. This requires the introduction of the distance between two distribution functions. We define the distance $d(f_\epsilon, f_0)$ as

$$d[f_\epsilon(t), f_0] = \left(\sum_{mn} |a_{\epsilon,mn} - a_{0,mn}|^2\right)^{1/2}. \tag{18}$$

## IV. HMF MODEL

### A. Equations of motion

The HMF model [6,7,12] is a continuous time model of globally coupled particles. Particle dynamics has been shown to have nontrivial collective features [13] and thermodynamical properties that pertain to a large class of long-range interacting systems [6,7,14–19]. The model describes $N$ particles on a circle with coordinates $-\pi \le x \le \pi$, momenta $p \in \mathbb{R}$, and the "magnetization" $\mathbf{m}(x)=(\cos x, \sin x)$. Particles interact via the mean magnetization $\langle\mathbf{m}\rangle = N^{-1}\Sigma_i \mathbf{m}_i$, where $\mathbf{m}_i=\mathbf{m}(x_i)$. The HMF Hamiltonian is

$$H(\{x_i,p_i\}_{i=1}^N) = \sum_{i=1}^N \frac{p_i^2}{2} + \frac{1}{2N}\sum_{i,j=1}^N [1 - \mathbf{m}_i\cdot\mathbf{m}_j]. \tag{19}$$

It defines $N$-particle dynamics by

$$\frac{d^2x_i}{dt^2} + \langle\mathbf{m}\rangle \wedge \mathbf{m}_i = 0. \tag{20}$$

In the limit $N\to\infty$, fixed energy per particle $U=H/N$,

$$U = \frac{1}{2}\langle p^2\rangle + \frac{1 - |\langle\mathbf{m}\rangle|^2}{2}, \tag{21}$$

correlations between particles yield to the collective phenomena. In this collisionless limit, the Vlasov equation for the HMF assumes the form

$$\frac{\partial f}{\partial t} + p\frac{\partial f}{\partial x} - \mathbf{m}_f(t)\wedge\mathbf{m}(x)\frac{\partial f}{\partial p} = 0. \tag{22}$$

The mean-field magnetization is defined by $\mathbf{m}_f(t)=\int\mathbf{m}(x)f(x,p,t)dxdp$.

### B. Homogeneous stationary states

We consider a two-parameter family of homogeneous $(\mathbf{m}_f=0)$ distributions $f_0(p;\alpha,\beta)$ given by

$$f_0(p;\alpha,\beta) = \frac{1}{2\pi w_p}\frac{1}{1+\exp(\beta p^2/2 - \alpha)}. \tag{23}$$

This form of distribution is a special case of a class of distributions, defined by $f\sim[1+\exp(\beta H-\alpha)]^{-1}$, shown to be important in the statistical treatment of the "violent relaxation" processes [20]. Their relevance to the HMF model has been discussed in [16].

Assuming that $f_0$ is normalized, $\int f_0(p)dp=2\pi$, the parameters $\alpha$, $\beta$ are related to $w_p$, $U$ by the self-consistency conditions [21]: $\beta w_p^2 = 2\pi[F_{-1/2}(\alpha)]^2$, $U=F_{1/2}(\alpha)/2\beta F_{-1/2}(\alpha)+1/2$. Three examples of $f_0(p;\alpha,\beta)$ for different values of $U$ are shown in Fig. 1.

The effective temperature $\hat{\beta}$, determined by Eq. (11), is

$$\hat{\beta} = \frac{\beta F_{-1/2}(\alpha)}{F_{1/2}(\alpha)}, \tag{24}$$

where

$$F_j(\alpha) = \frac{1}{\Gamma(j+1)}\int_0^\infty \frac{t^j}{\exp(t-\alpha)+1}$$

are the standard Fermi-Dirac integrals.

In Ref. [21], it has been demonstrated that, in the parameter plane $(w_p, U)$, the stable and the unstable stationary states [Eq. (23)] are separated by the boundary curve

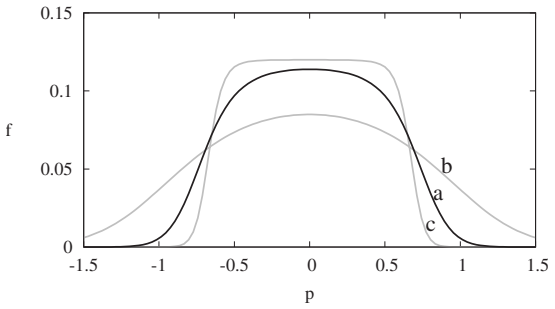


FIG. 1. Several homogeneous stationary states $f_0(p;\alpha,\beta)$, corresponding to fixed $w_p=1.3262$. Energies are $U_a=0.6$, $U_b=0.72$, and $U_c=0.577$ (see also Fig. 4).

$\ell_c(\alpha)=[w_{p,c}(\alpha),U_c(\alpha)]$. Defining $G_j(x,\alpha)$ for $\alpha\in\mathbb{R}$ and $x\in\mathbb{R}^+$ by

$$G_j(x,\alpha)=\frac{1}{\Gamma(j+1)}\int_0^\infty \frac{\exp(t-\alpha)}{[1+\exp(t-\alpha)]^2}\frac{t^{j+1}dt}{t+x}, \quad (25)$$

we express $\ell_c$ as

$$\ell_c(\alpha)=\left([\pi F_{-1/2}(\alpha)G_{-1/2}(0,\alpha)]^{1/2},\ \frac{F_{1/2}(\alpha)G_{-1/2}(0,\alpha)}{4[F_{-1/2}(\alpha)]^2}+\frac{1}{2}\right). \quad (26)$$

In Ref. [21] it has also been demonstrated that for a fixed value of $w_p$, $U\geq U_{\min}(w_p)=1/2+w_p^2/24$. This defines the limiting boundary curve $\ell_{\min}(w_p)=(w_p,w_p^2/24+1/2)$. Note that approaching $\ell_{\min}$ corresponds to taking the asymptotic limit of $\alpha\to\infty$ of the distribution function [Eq. (23)]. In this limit $f_0$ tends to the "water-bag" distribution defined by $f_{\rm wb}(p)=(2\pi w_p)^{-1}\Theta(|p|-w_p/2)$, where $\Theta(p)$ is the Heaviside function. Close to this boundary, differentiability properties of $f_0$ deteriorate and the convergence of the coefficient expansion is slower.

In the following we will compare our calculations of Lyapunov exponents with results on phase transitions for the HMF model, discussed in Refs. [16,21].

Figure 2 shows the divergence from equilibrium of a perturbed homogeneous stationary state, corresponding to the curve (a) in Fig. 1. The evolution has been obtained by numerical integration of Eq. (20). The initial exponential divergence is clearly displayed, together with the subsequent saturation to a quasistationary state, characterized by low-frequency oscillations. The inset of Fig. 2 shows the system dynamics, projected in coefficients $[a_{0,2},\mathrm{Re}(a_{1,1}),\mathrm{Im}(a_{1,2})]$. As it can be seen, the stretch of the (almost linear) initial trajectory, slightly bending toward the attractor just before the reference point at $t=20$, shows the qualitative features of the long-term dynamics.

## V. RESULTS AND DISCUSSION

Linearization of the Vlasov equation [Eq. (1)] around the family of distributions [Eq. (23)] shows that the Lyapunov spectrum consists of a continuum of real eigenvalues, associated with spectrally stable modes, as well as a finite number of imaginary eigenvalues, to be associated with unstable

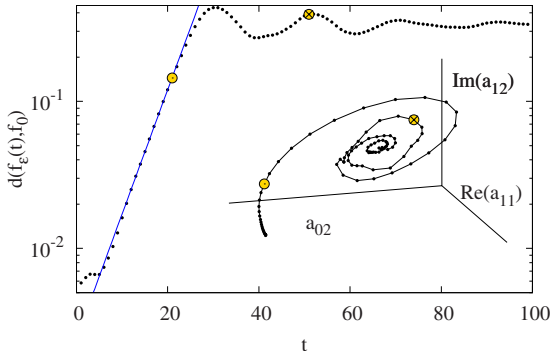


FIG. 2. (Color online) Temporal evolution of a perturbation of the stationary state (a) of Fig. 1, represented by the distance [Eq. (18)] and by a trajectory in the coefficient $[a_{0,2},\mathrm{Re}(a_{1,1}),\mathrm{Im}(a_{1,2})]$ space (inset.) The thick open circle marks the state at $t=20$, while the thick crossed circle marks the state at $t=50$. The fit of the exponential regime predicts $\lambda=0.1947\pm0.0013$. The stationary state (a) is used as the probability density to randomly generate the initial coordinates and momenta for $N=10^6$ particles, and the finite number of particles is used to mimic the initial perturbation of the stationary state. The initial conditions were evolved by integrating Eq. (20).

collective modes. In the case of homogeneous distributions, Lyapunov exponents of the collective modes can be expressed succinctly, using the plasma dispersion function $\varepsilon(\sigma)$, as an equation $\varepsilon(\sigma)=0$ [3,4]. The plasma dispersion function for the HMF model has been derived in [7],

$$\varepsilon(\sigma)=1+\pi\int_{-\infty}^{\infty}\frac{1}{p+\sigma}\frac{\partial f_0(p)}{\partial p}dp, \quad (27)$$

where $f_0$ is given by Eq. (23). The boundary between stable and unstable stationary states is determined by $\varepsilon(0)=0$. The result is the curve $\ell_c$, given by Eq. (26). The local (real and positive) Lyapunov exponent $\lambda$ is found as a solution of $\varepsilon(\iota\lambda)=0$. We define this solution as the Lyapunov map,

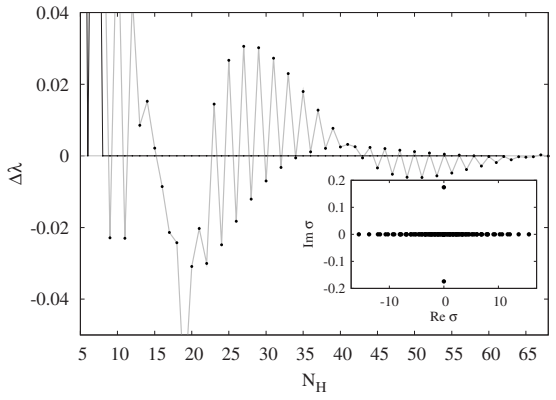


FIG. 3. The difference $\Delta\lambda$ between the largest Lyapunov exponent [Eq. (16)] and the exact value [Eq. (28)] as a function of the truncation order $N_H$ in Hermite polynomials. Here $N_F=5$. Two cases are shown: the unstable state (a) (dotted line) and the stable state (b) (continuous line). The inset shows the complete Lyapunov spectrum of the unstable state (a).

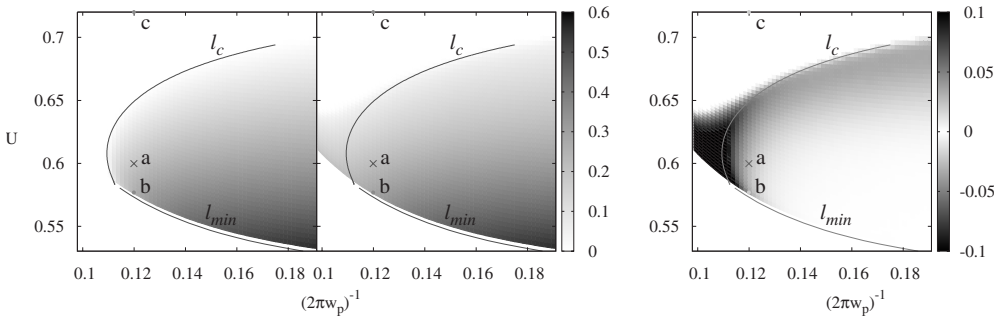


FIG. 4. Comparison between the exact Lyapunov map and computation using the truncated spectral equation [Eq. (29)]. The left panel shows the Lyapunov map [Eq. (28)]. The middle panel shows the computation using Eq. (29) with $N_F=5$ and averaging over $N_H$ between 31 and 61. Their difference is shown in the right panel. Letters indicate special values of parameters, discussed in this paper.

$$\lambda(w_p,U)=\sqrt{\frac{2}{\beta}G_{-1/2}^{-1}\left(\frac{2F_{-1/2}(\alpha)}{\beta},\alpha\right)}, \tag{28}$$

where $G_j^{-1}(x,\alpha)$ is the inverse of $G_j(x,\alpha)$ [given by Eq. (25)] with respect to the variable $x$, while $\alpha=\alpha(w_p,U)$ and $\beta=\beta(w_p,U)$ are expressed in terms of $w_p$ and $U$ using the self-consistency conditions.

For nonhomogeneous stationary distributions, the dispersion relation does not have a closed form, such as Eq. (27), and solving Eq. (13) is the only direct way to obtain the Lyapunov spectrum. Equation (13) specialized for the HMF model reads

$$\sigma\psi_{m,n}=m\left(\frac{\psi_{m,n-1}}{\hat{\beta}}+(n+1)\psi_{m,n+1}\right)+\sum_{k=\pm1}\frac{k}{2}[a_{k,0}\psi_{m-k,n-1}+a_{m-k,n-1}\psi_{k,0}]. \tag{29}$$

Figure 3 shows the difference between the Lyapunov exponent [Eq. (16)] and the exact value [Eq. (28)] as a function of the truncation order $N_H$ in Hermite polynomials. The number of Fourier modes is fixed at $N_F=5$. Two cases are shown, corresponding to the unstable state (a) (exact value $\lambda_a=0.189\,549$) and to the stable state (b) ($\lambda_b=0$) in Fig. 1. As it can be seen, $N_H\geq 7$ allows us to predict real Lyapunov spectrum of the stationary state (b) and to predict a positive Lyapunov exponent of the unstable stationary state (a) qualitatively. Given that the sources of errors include both the finite truncation error and errors in the approximation of the coefficients (computed using Monte Carlo integration), the convergence to the exact value $\lambda_a$ can be considered as satisfactory. The inset of Fig. 3 shows the complete Lyapunov spectrum of the unstable state (a), including a single local Lyapunov exponent. All remaining eigenvalues have a vanishing imaginary part and tend to cover the real axis densely.

In Fig. 4 we display the Lyapunov map $\lambda(w_p,U)$. The exact map [Eq. (28)], the approximation computed via Eq. (29), and their difference are shown in the left, center, and right panels, respectively. The center panel was computed by averaging the largest Lyapunov exponent over the order of truncation, $N_H$, between $N_H=31$ and $N_H=61$ and with the fixed $N_F=5$. The agreement is fully satisfactory for the high-energy stable stationary states. Indeed, consistently with what is reported in Fig. 3, we have verified that for $N_H\geq 7$ the computed Lyapunov spectrum by Eq. (29) in this region is always real, and therefore predictions of spectral stability are unambiguous. Similarly, apart from the region close to the intersection between $\ell_{\min}$ and $\ell_c$, one can see that also the unstable states are predicted unambiguously. The largest Lyapunov exponent converges to the exact value as the truncation size is increased. As for the error in the intersection region, analysis, similar to the one shown in Fig. 3, demonstrates that close to $\ell_c$ the prediction of $\lambda$ is more sensitive to errors in the coefficients $a_{0,mn}$. Moreover, deterioration of results computed with a fixed truncation order $N_H$ close to

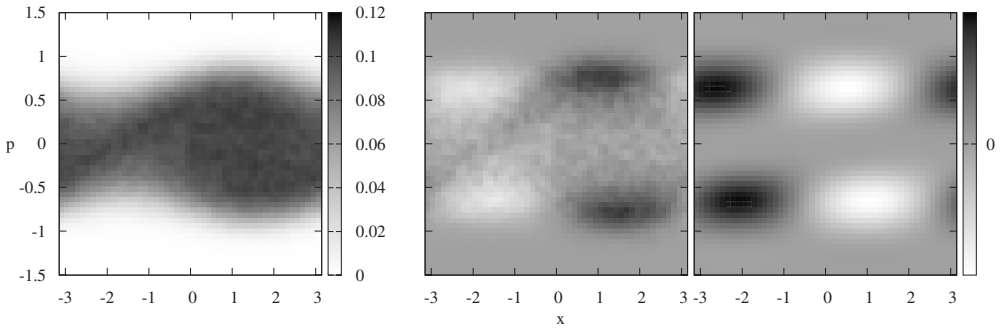


FIG. 5. Exponential amplification of a perturbed stationary state (a) as given by Eq. (17). The left panel shows the distribution $f(t)$ at $t=20$ (indicated by a thick dot in Fig. 2). The center panel shows the difference between $f(20)$ and the initial distribution. The right panel shows the expanding eigenvector, corresponding to $\lambda_a$, computed using Eq. (29) with $N_F=5$, $N_H=11$.

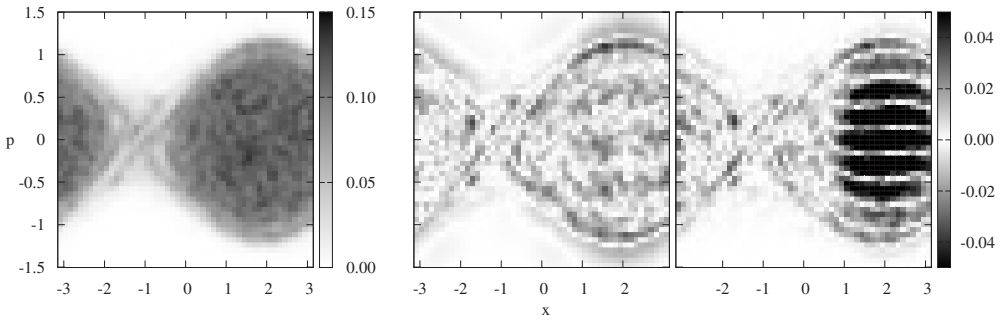


FIG. 6. The left panel shows the reference distribution $f(t)$ at $t=50$, at which time the effective temperature [Eq. (10)] is $T\approx 1/3.5$. The center and the right panels show the difference between the reference distribution and the Fourier-Hermite expansion [Eq. (4)], with $\hat{\beta}=3.5$ and $\hat{\beta}=10$, respectively. In both cases $N_F=5$, $N_H=11$. The point of reference $t=50$ is also indicated by a thick crossed circle in Fig. 2.

$\ell_{\min}$ can be anticipated because of differentiability properties of $f_0$.

For comparison, the exact Lyapunov exponent for the state (a) $\lambda_a=0.1895$. Simulation of $1\times 10^6$ particles (see Fig. 2) gives $\lambda=0.1947$. The convergence to $\lambda_a$ of the calculation based on Fourier-Hermite expansion is displayed in Fig. 3. On can see that our method is in good agreement with both the $N$-body simulation and the exact calculation.

The full solution of Eq. (13) provides detailed information about local directionality of transitions associated to each eigenvalue. In the presence of a single positive local Lyapunov exponent or if one local Lyapunov exponent is larger than the remaining ones, this directionality is expressed by Eq. (17). To test accuracy of our method with respect to calculation of expanding eigenvectors, in Fig. 5 we explore the temporal divergence of a perturbed stationary state (a). Direct numerical integration of Eq. (20) up to $t=20$, i.e., close to breakdown of the regime of exponential divergence (see Fig. 2), results in the distribution, shown in the left panel of Fig. 5. Subtraction of the initial state from the latter is shown in the central panel. A direct comparison with the unstable expanding mode, calculated using truncated Eq. (29) with $N_F=11$, $N_H=5$ (see the right panel), demonstrates that also Lyapunov eigenvectors are predicted accurately.

As a final step, we tested the ability of our method to represent the distribution function, with $\hat{\beta}$ tuned to the inverse temperature, after the exponential regime, i.e., outside the limit of validity of Eq. (29). Results are summarized in Fig. 6. Considering again the perturbed stationary state (a), distribution at $t=50$ is shown in the left panel of Fig. 6 (indicated by a thick crossed circle in Fig. 2). The effective temperature of the distribution is $T\approx 1/3.5$. The difference between a representation using fixed low-order truncation $(N_F=5, N_H=11)$ is shown in the center panel for $\hat{\beta}=3.5$ and in the right panel for $\hat{\beta}=10$. As it can be seen, the case in which $\hat{\beta}$ is tuned at the inverse of the system temperature results in smaller errors of the approximation. The agreement using a detuned $\hat{\beta}$ can be improved by increasing the order of the Hermite expansion.

## VI. CONCLUSIONS

We have proposed an efficient method to compute Lyapunov exponents and Lyapunov eigenvectors of collective states in long-range interacting many-particle systems, whose dynamics is described by the Vlasov equation. The method is based on expanding the distribution function in a Fourier-Hermite basis, with a scaled momentum variable. Having tuned the scaling parameter to maximize the content of the lowest order coefficient of the expansion, we have demonstrated that the Lyapunov exponent and Lyapunov eigenvectors converge fast to the values predicted by direct $N$-body simulations and by exact analytical calculations. As an example of a long-range interacting system we have considered the Hamiltonian mean-field model. We have investigated stability properties of a two-parameter family of homogeneous distributions over a wide range of dynamical conditions. Our conclusion is that linear stability properties and dynamics of long-range interacting systems can be represented and computed using a small number of modes and thus a small numerical effort.

[1] J. H. Jeans, Mon. Not. R. Astron. Soc. **76**, 70 (1915).
[2] A. Vlasov, *Many-Particle Theory and Its Application To Plasma* (Gordon and Breach, New York, 1961).
[3] D. Bohm and E. P. Gross, Phys. Rev. **75**, 1851 (1949).
[4] R. Balescu, *Statistical Dynamics: Matter Out of Equilibrium* (Imperial College Press, London, 1997).
[5] H. Poincaré, *New Methods of Celestial Mechanics* (American Institute of Physics, New York, 1993), Pt. 3.
[6] S. Inagaki, Prog. Theor. Phys. **90**, 577 (1993).
[7] M. Antoni and S. Ruffo, Phys. Rev. E **52**, 2361 (1995).
[8] B. Fornberg, *A Practical Guide to Pseudospectral Methods (Number 1 in Cambridge Monographs on Applied and Computational Mathematics)* (University Press, Cambridge, 1995).
[9] J. W. Schumer and J. P. Holloway, J. Comput. Phys. **144**, 626

(1998).
[10] T. P. Armstrong, Phys. Fluids **10**, 1269 (1967).
[11] F. C. Grant and M. R. Feix, Phys. Fluids **10**, 696 (1967).
[12] *Dynamics and Thermodynamics of Systems with Long-Range Interactions: An Introduction*, Lecture Notes in Physics Vol. 602, edited by T. Dauxois, S. Ruffo, E. Arimondo, and M. Wilkens (Springer, Berlin, 2002).
[13] H. Morita and K. Kaneko, Phys. Rev. Lett. **96**, 050602 (2006).
[14] Y. Y. Yamaguchi, J. Barré, F. Bouchet, T. Dauxois, and S. Ruffo, Physica A **337**, 36 (2004).
[15] J. Barré, F. Bouchet, T. Dauxois, S. Ruffo, and Y. Y. Yamaguchi, Physica A **365**, 177 (2006).
[16] A. Antoniazzi, D. Fanelli, J. Barre, P. H. Chavanis, T. Dauxois, and S. Ruffo, Phys. Rev. E **75**, 011112 (2007).
[17] V. Latora, A. Rapisarda, and S. Ruffo, Physica D **131**, 38 (1999).
[18] Y. Y. Yamaguchi, F. Bouchet, and T. Dauxois, J. Stat. Mech.: Theory Exp. (2007), P01020.
[19] A. Antoniazzi, F. Califano, D. Fanelli, and S. Ruffo, Phys. Rev. Lett. **98**, 150602 (2007).
[20] D. Lynden-Bell, Mon. Not. R. Astron. Soc. **136**, 101 (1967).
[21] P. H. Chavanis, Eur. Phys. J. B **53**, 487 (2006).